

New carbon-nitrogen-oxygen compounds as high energy density materials

Junyu Shen(沈俊宇), Qingzhuo Duan(段青卓), Junyi Miao(苗俊一), Shi He(何适), Kaihua He(何开华), Wei Dai(戴伟), and Cheng Lu(卢成)

Citation: Chin. Phys. B, 2023, 32 (**9**): 096302. DOI: 10.1088/1674-1056/acce94
Journal homepage: http://cpb.iphy.ac.cn; http://iopscience.iop.org/cpb

What follows is a list of articles you may be interested in

Boron at tera-Pascal pressures

Peiju Hu(胡佩菊), Junhao Peng(彭俊豪), Xing Xie(谢兴), Minru Wen(文敏儒),Xin Zhang(张欣), Fugen Wu(吴福根), and Huafeng Dong(董华锋)

Chin. Phys. B, 2022, 31 (**3**): 036301. DOI: 10.1088/1674-1056/ac11e6

Superconductivity in electron-doped arsenene

Xin Kong(孔鑫), Miao Gao(高淼), Xun-Wang Yan(闫循旺), Zhong-Yi Lu(卢仲毅), Tao Xiang(向涛)

Chin. Phys. B, 2018, 27 (**4**): 046301. DOI: 10.1088/1674-1056/27/4/046301

High-pressure dynamic, thermodynamic properties, and hardness of CdP_2

Shi-Quan Feng(冯世全), Ling-Li Wang(王伶俐), Xiao-Xu Jiang(姜晓旭), Hai-Nin Li(李海宁), Xin-Lu Cheng(程新路), Lei Su(苏磊)

Chin. Phys. B, 2017, 26 (**4**): 046301. DOI: 10.1088/1674-1056/26/4/046301

Lattice stabilities, mechanical and thermodynamic properties of Al_3Tm and Al_3Lu intermetallics under high pressure from first-principles calculations

Xu-Dong Zhang(张旭东) and Wei Jiang(姜伟)

Chin. Phys. B, 2016, 25 (**2**): 026301. DOI: 10.1088/1674-1056/25/2/026301

High-pressure phonon dispersion of copper by using the modified analytic embedded atom method

Zhang Xiao-Jun (张晓军), Chen Chang-Le (陈长乐), Feng Fei-Long (凤飞龙)

Chin. Phys. B, 2013, 22 (**9**): 096301. DOI: 10.1088/1674-1056/22/9/096301

New carbon–nitrogen–oxygen compounds as high energy density materials

Junyu Shen(沈俊宇)[1], Qingzhuo Duan(段青卓)[1], Junyi Miao(苗俊一)[1], Shi He(何适)[2], Kaihua He(何开华)[1], Wei Dai(戴伟)[3], and Cheng Lu(卢成)[1,†]

[1] *School of Mathematics and Physics, China University of Geosciences (Wuhan), Wuhan* 430074, *China*
[2] *Faculty of Materials Science and Chemistry, China University of Geosciences (Wuhan), Wuhan* 430074, *China*
[3] *School of Mathematics and Physics, Jingchu University of Technology, Jingmen* 448000, *China*

(Received 8 April 2023; revised manuscript received 8 April 2023; accepted manuscript online 20 April 2023)

Molecular crystals are complex systems exhibiting various crystal structures, and accurately modeling the crystal structures is essential for understanding their physical behaviors under high pressure. Here, we perform an extensive structure search of ternary carbon-nitrogen-oxygen (CNO) compound under high pressure with the CALYPSO method and first principles calculations, and successfully identify three polymeric CNO compounds with *Pbam*, $C2/m$ and $I\bar{4}m2$ symmetries under 100 GPa. More interestingly, these structures are also dynamically stable at ambient pressure, and are potential high energy density materials (HEDMs). The energy densities of *Pbam*, $C2/m$ and $I\bar{4}m2$ phases of CNO are about 2.30 kJ/g, 1.37 kJ/g and 2.70 kJ/g, respectively, with the decompositions of graphitic carbon and molecular carbon dioxide and α-N (molecular N_2) at ambient pressure. The present results provide in-depth insights into the structural evolution and physical properties of CNO compounds under high pressures, which offer crucial insights for designs and syntheses of novel HEDMs.

Keywords: molecular crystals, high pressure, structure searches, first principles calculations, high energy density materials

PACS: 63.20.dk, 31.15.E–, 71.20.–b **DOI:** 10.1088/1674-1056/acce94

Molecular crystals are a type of important solid-state materials in which constituent molecules are arranged in a regular, repeating pattern to form a crystal lattice. The stabilities and chemical bonding characteristics of molecular crystals are determined by the types of molecules, the crystal structures and symmetries, as well as intermolecular interactions between the molecules. For instance, under ambient conditions, molecular nitrogen gas, N_2, is highly stable and inert due to the strong N≡N triple bond between N atoms, characterized by a bond length of 1.10 Å and a dissociation energy of 954 kJ/mol.[1] At pressures more than 110 GPa,[2–4] N–N single bonds become the preferred forms. The N≡N triple bond is much stronger than the N=N double bond (418 kJ/mol) or the N–N single bond (160 kJ/mol),[5] and the decomposition of polymeric nitrogen bonded by the single bond can release a large amount of energies. In principle, solid nitrogen and nitrogen-based compounds are promising candidates of high energy density materials (HEDMs). High pressure[2,3,6–8] is an effective method to break the extremely strong N≡N triple bonds and to yield polymeric nitrogen compounds with N–N single bonds.[9,10] In fact, many kinds of polymeric nitrogen, such as cg-N, LP-N and HLP-N are observed under high pressure.[11] However, it is still a challenge to release these high-pressure phases of nitrogen to be metastable under ambient conditions. Considering the harshness of synthetic conditions and the desirable energetic properties of polymeric nitrogen compounds,[12–17] it is still necessary to find new nitrogen-containing compounds.

One feasible avenue is to synthesize nitrogen-containing compounds through high pressure, and then release pressure to ambient pressure and stabilize them. Another possible way to achieve polymerized nitrogen compounds under ambient conditions is the combination of nitrogen with other elements through chemical pre-compression.[18–21] These processes can promote formation of polymeric nitrogen compounds and stabilize them under relatively low pressure or ambient pressure. Carbon (C), nitrogen (N) and oxygen (O) are essential elements on the Earth. They are highly abundant and readily available, and numerous compounds comprising these elements have been verified as HEDMs,[22,23] for example, carbon monoxide, nitrogen dioxide and dinitrogen pentoxide. The bond energies of multiple bonds in these compounds are 256.5 kcal/mol (C≡O triple bond), 145.0 kcal/mol (N=O double bond), and 114.0 kcal/mol (N=O double bond), and the bond energies of single bonds of these elements in different compounds are about 84.0–131.0 kcal/mol (C–O single bond) and 48.0–84.0 kcal/mol (N–O single bond). In fact, several compounds such as OCNNO, $CNNO_2$, and $NCNO_2$ are experimentally synthesized.[6,12] Although significant progress has been made by numerous researchers in recent years, a comprehensive understanding of the structural and chemical bonding characteristics relevant to the polymerization and decomposition processes of nitrogen compounds containing C and O is essential for gaining deeper insight into explosive properties

[†]Corresponding author. E-mail: lucheng@calypso.cn

© 2023 Chinese Physical Society and IOP Publishing Ltd

of C–N–O systems.

In this work, we conduct an extensive structure search for C–N–O systems at different pressures via the CALYPSO method combined with first principles calculations.[24,25] Our findings indicate that nitrogen can readily react with carbon and oxygen at relatively low pressures (approximately 40 GPa) to form HEDMs with different compositions. We then focus on the stoichiometry of carbon-nitrogen-oxygen (CNO) compounds, and successfully identify the *Pbam* phase of CNO under 100 GPa, along with two novel polymeric CNO compounds possessing $C2/m$ and $I\bar{4}m2$ symmetries. These three polymeric CNO compounds are potential HEDMs with energy densities of 2.30 kJ/g for *Pbam* phase, 1.37 kJ/g for $C2/m$ phase, and 2.70 kJ/g for $I\bar{4}m2$ phase.

Table 1. Calculated elastic constants C_{ij} (GPa) of CNO under ambient pressure and 100 GPa.

Pressure	Phase	C_{11}	C_{22}	C_{33}	C_{44}	C_{55}	C_{66}	C_{12}	C_{13}	C_{15}	C_{23}	C_{25}	C_{35}	C_{46}
0 GPa	*Pbam*	871	843	1432	164	403	514	278	174	–	60	–	–	–
	$C2/m$	728	1454	1266	97	426	248	152	272	−72	−28	−58	28	−80
	$I\bar{4}m2$	809	–	30	6	–	97	−33	1	–	–	–	–	–
100 GPa	*Pbam*	515	550	1502	118	148	189	226	114	–	694	–	–	–
	$C2/m$	728	1454	1266	97	426	249	152	272	−72	−28	−58	28	−80
	$I\bar{4}m2$	1572	–	990	305	–	136	−57	209	–	–	–	–	–

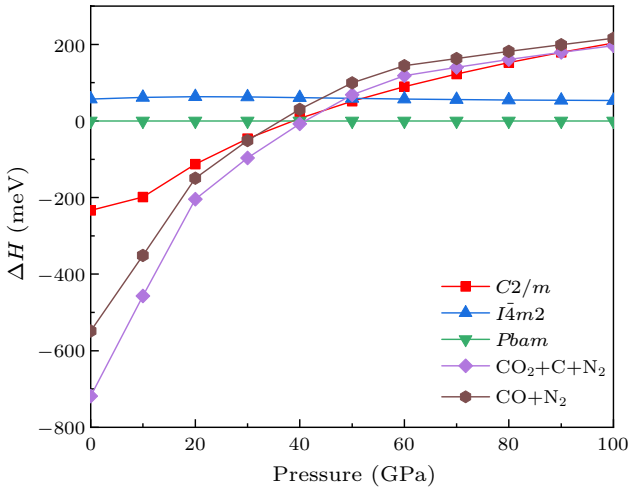


Fig. 1. Calculated enthalpy differences relative to the *Pbam* phase for the CNO compound under high pressure from 0 to 100 GPa.

We have employed the CALYPSO method and first-principles calculations to predict the crystal structures of C–N–O systems at ambient pressure, 50 GPa, and 100 GPa.[24,25] For each stoichiometry and pressure, we have conducted approximately 50 generations of structure searches with 30 different conformational geometries in each generation, and identified approximately 1500 distinct structures for the CNO compound. We have used the Vienna *ab initio* simulation package (VASP)[26] through the framework of density function theory (DFT)[27–29] combined with projector augmented-wave pseudopotentials and generalized gradient approximation with Perdew–Burke–Ernzerhof exchange correlation functions[30] to optimize the total energy of all predicted structures. To ensure the convergence of energy and forces to less than 1 meV/atom and 0.001 eV/Å, we have adopted a dense k-point of $2\pi \times 0.025$ for the Brillouin zone integral and an energy cutoff of 800 eV. The mechanical stabilities of the predicted structures are evaluated via elastic constants calculated using the strain-stress method. The dynamic stabilities of each low-energy structure is assessed using phonon dispersion curves simulated by the PHONOPY code.

The calculated enthalpies of the CNO compound under high pressure are illustrated in Fig. 1. As shown in Fig. 1, the CNO system undergoes the decomposition into $CO_2 + C + N_2$ combinations at pressures below 40 GPa. However, the *Pbam*, $C2/m$, and $I\bar{4}m2$ phases of CNO exhibit stable phases at pressures exceeding 50 GPa. Notably, the energy of the $C2/m$ structure is found to be lower in energy than that of the *Pbam* structure reported by Raza *et al.*,[1] suggesting that the energy characteristics of the $C2/m$ phase is superior to that of the *Pbam* phase. In the following, we will elaborate on the underlying mechanism.

At ambient pressure, the CNO system is decomposed into $CO_2 + C + N_2$ components. However, the high-pressure phases of *Pbam*, $C2/m$, and $I\bar{4}m2$ structures are dynamically stable with weak van der Waals interactions. To exactly describe the structural and explosive properties of the CNO compound, we consider the DFT-D2 van der Waals corrections in the present calculations. In the *Pbam* phase of CNO, the crystal structure is a layered geometry consisting of CN_2O_2 tetrahedra with one C atom in the center. The optimized lattice constants are $a = 8.390$ Å, $b = 4.019$ Å, $c = 2.431$ Å, $\alpha = 90.000°$, $\beta = 90.000°$, and $\gamma = 90.000°$, respectively. The coordination numbers of C, N, and O atoms are 4, 3, and 2, respectively. The C–O bond lengths are found to be 1.437 Å and 1.419 Å, while the C–N bond length is 1.462 Å. The N–N bond length is 1.430 Å, which is longer than the typical bond length of N–N single bond (1.30 Å). For the $C2/m$ structure, there are six atoms per unit cell, and the calculated structural parameters are $a = 12.642$ Å, $b = 2.280$ Å, $c = 2.273$ Å, $\alpha = 90.000°$, $\beta = 79.625°$, and $\gamma = 90.000°$. The coordination numbers of C, N, and O atoms are 4, 3, and 2, respectively. The C–O bond lengths are 1.450 Å and 1.364 Å, and the C–N bond length is 1.387 Å, while the N–N bond length is 1.360 Å, which is longer than the 1.30 Å N–N single bond length. In the $I\bar{4}m2$ phase of CNO, the predicted lattice constants are

$a = b = 2.401$ Å, $c = 15.583$ Å, $\alpha = 90.000°$, $\beta = 90.000°$, and $\gamma = 90.000°$. The C atoms are coordinated by two O atoms and two N atoms, while the N atoms are coordinated by two C atoms and one N atom, and the O atoms are coordinated by two C atoms. The bond length of C–O is found to be 1.472 Å, which is longer than the C–N bond length of 1.449 Å. The N–N bond length is 1.349 Å, which is greater than the 1.30 Å of the N–N single bond length. As such, the N atoms in the $I\bar{4}m2$ phase of CNO exist in the form of single bonds.

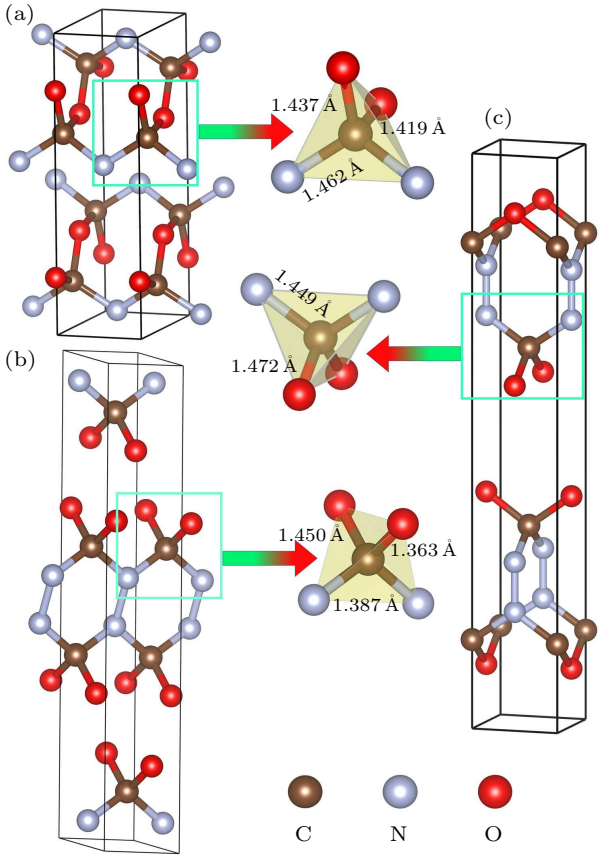


Fig. 2. Crystal structures of the CNO compound at ambient pressure: (a) *Pbam* phase, (b) $C2/m$ phase, and (c) $I\bar{4}m2$ phase. The local tetrahedra of CNO units are illustrated for each structures. The red, brown and gray balls are oxygen, carbon and nitrogen atoms, respectively.

To confirm the dynamical stability of the CNO, we have performed phonon spectra calculations of CNO under different pressures, and the results are presented in Fig. 3. The phonon dispersions of all three structures are stable under high pressure and ambient pressure, indicating dynamically stable CNO. The calculated results of *Pbam* phase of CNO are consistent with those reported by Raza *et al.*,[1] validating the reliabilities of current calculations. Additionally, the results of the electron localization function calculations of CNO reveal that both $C2/m$ and $I\bar{4}m2$ structures exhibit typical δ bonds[31] between the C and N atoms and the C and O atoms, as well as localized electrons at the peripheries of the O and N atoms. To verify the mechanical stability of CNO, we have used the *ab initio* stress-strain relation method to calculate the elastic constants of CNO under different pressures.

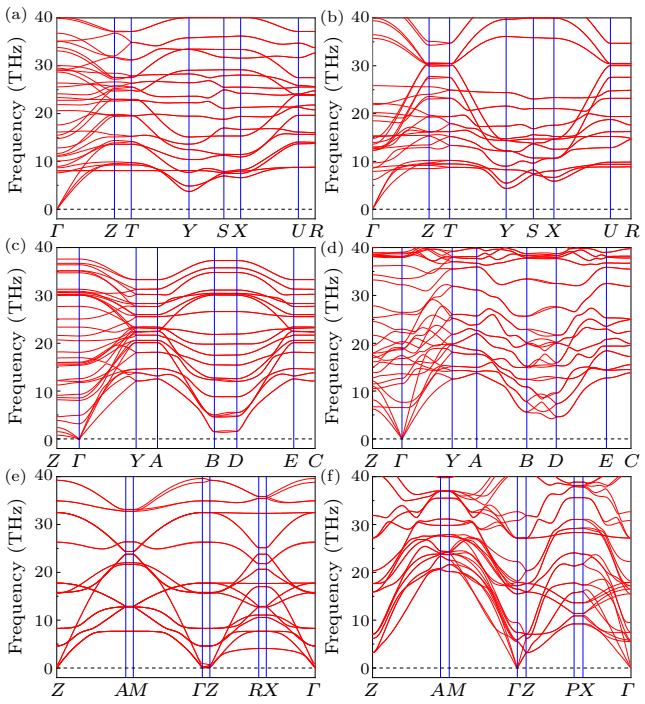


Fig. 3. Phonon dispersion curves of CNO under different pressures: (a) *Pbam* phase at ambient pressure, (b) *Pbam* phase at 100 GPa, (c) $C2/m$ phase at ambient pressure, and (d) $C2/m$ phase at 100 GPa, (e) $I\bar{4}m2$ phase at ambient pressure, (f) $I\bar{4}m2$ phase at 100 GPa.

Table 2. The Bader charge analysis of CNO compounds at ambient pressure.

Phase	C	N	O
Pbam	−1.55	0.65	0.95
$C2/m$	−1.23	0.28	0.95
$I\bar{4}m2$	−1.43	0.63	0.80

The calculated results are summarized in Table 1. It can be seen from Table 1 that the calculated results are perfectly satisfied with mechanical stability criteria of orthorhombic, tetragonal, and monoclinic crystals.[32] Thus, these structures are mechanically stable at ambient pressure and 100 GPa.

Based on calculations of the energy band and electronic density of states (DOS), we have found that the *Pbam*, $C2/m$, and $I\bar{4}m2$ phases of CNO exhibit semiconducting behavior, with corresponding band gap values of 3.18 eV, 1.59 eV, and 1.32 eV, respectively. The DOSs of *Pbam* and $C2/m$ phases of CNO at ambient pressure reveal that the N atoms make significant contributions to the electronic states below the Fermi level, with clear evidence of orbital hybridizations observed in all three phases. Similarly, the DOSs of the $I\bar{4}m2$ phase of CNO at ambient pressure show that the N and O atoms have higher contributed values below the Fermi level. In all cases, the DOSs below the Fermi energy level are found to be dominated by C-sp, N-sp, and O-sp orbitals, indicating the presence of strong C–N, C–O, and N–N chemical bonds. Additionally, we have performed Bader charge calculations to analyze the charge transfer behaviors between different elements in CNO. The results are listed in Table 2. In the $I\bar{4}m2$ structure of CNO, the Bader charge analysis[33] shows that C atoms donate about

0.63e to the N atoms and 0.80e to the O atoms. In contrast, for the $C2/m$ structure of CNO, the transferred electron numbers of 0.95e from C atoms to O atoms are much larger than that to N atoms, with a value of approximately 0.30e. Based on the results of the Bader charge transition analysis, it can be concluded that the chemical bonds in the $I\bar{4}m2$ structure of CNO are stronger than those in the $C2/m$ structure, which suggest that the energy density of the $I\bar{4}m2$ structure is higher than that of the $C2/m$ structure.

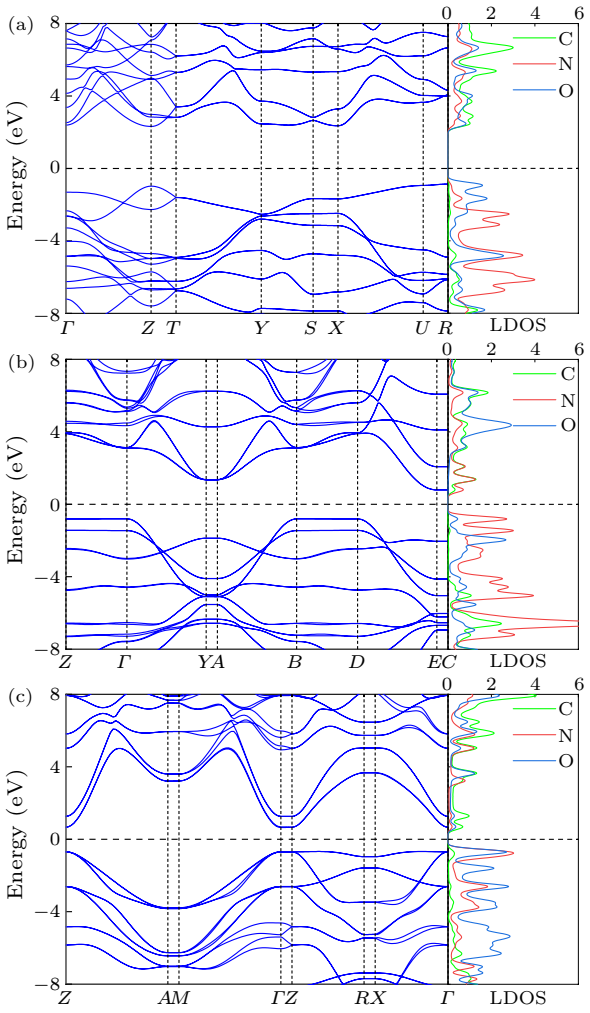


Fig. 4. Electronic properties of CNO at ambient pressure: (a) energy band and DOS of the *Pbam* phase, (b) energy band and DOS of the $C2/m$ phase, and (c) energy band and DOS of the $I\bar{4}m2$ phase.

In order to gain deeper understanding of the interatomic bonding interactions of the three CNO phases, we have conducted a computational analysis of the crystal orbital Hamilton population (COHP)[34,35] for these structures. The COHP analysis partitions the energy band structure, expressed in terms of orbital pair contributions, into bonding, non-bonding, and anti-bonding energy regions within a specific energy range,[36] where positive values of -pCOHP indicate the bonding energy region, and negative values indicate the anti-bonding region. The COHP results are presented in Fig. 5. Notably, the $C2/m$ structure (Fig. 5(b)) exhibits weaker bonds compared to $I\bar{4}m2$ (Fig. 5(c)) and *Pbam* structures (Fig. 5(a)). Additionally, the significantly larger anti-bonding states are observed below E_f in the $C2/m$ phase, while the $I\bar{4}m2$ and *Pbam* phases lack this feature. These results are consistent with the enthalpy data for the $C2/m$, *Pbam*, and $I\bar{4}m2$ phases (shown in Fig. 1). The N–N bond in the $C2/m$ structure also displays an anti-bonding state, while no such feature is present in the $I\bar{4}m2$ and *Pbam* phases. By contrast, the strength of the C–N bonds in the three structures are not markedly different. Therefore, considering the limited number of N–N bonds, we infer that the stronger C–O bond is the primary factor contributing to the higher enthalpy of the corresponding CNO compound and resulting in the release of more energy during automatic decomposition under ambient pressure.

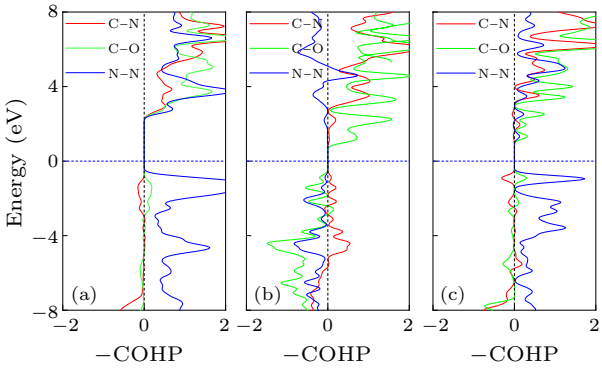


Fig. 5. Crystal orbital Hamilton population (pCOHP) analysis of CNO: (a) *Pbam* phase, (b) $C2/m$ phase, and (c) $I\bar{4}m2$ phase.

To evaluate the energy density of CNO, we decompress the three high pressure phases to ambient pressure and consider the following reaction equations:

$$4\mathrm{CNO}(Pbam) \rightarrow 2\mathrm{CO_2} + 2\mathrm{C} + 2\mathrm{N_2} + 4.01\ \mathrm{eV}$$
$$\text{(Production: cg-N)}$$
$$4\mathrm{CNO}(C2/m) \rightarrow 2\mathrm{CO_2} + 2\mathrm{C} + 2\mathrm{N_2} + 2.39\ \mathrm{eV}$$
$$\text{(Production: } \alpha\text{-N)}$$
$$4\mathrm{CNO}(I\bar{4}m2) \rightarrow 2\mathrm{CO_2} + 2\mathrm{C} + 2\mathrm{N_2} + 4.69\ \mathrm{eV}$$
$$\text{(Production: } \alpha\text{-N)}$$

where the three metastable phases of CNO are anticipated to undergo exothermic decomposition into carbon monoxide (graphitic carbon and molecular carbon dioxide) and α-N (molecular N_2) with solid carbon (graphitic carbon and molecular carbon dioxide). Using DFT calculations, we have calculated the chemical energies released during the decomposition reactions of CNO, which are 4.01 eV, 2.39 eV, and 4.69 eV for the *Pbam*, $C2/m$, and $I\bar{4}m2$ phases, respectively. Based on these values, we have estimated the energy densities per unit mass to be approximately 2.30 kJ/g, 1.37 kJ/g, and 2.70 kJ/g for the *Pbam*, $C2/m$, and $I\bar{4}m2$ phases, respectively.

In addition, we have also calculated these explosion parameters by our newly developed HEDPC method. The results are presented in Table 3. It can be seen from Table 3 that the

explosive properties of CNO are analogous to modern explosives TNT, HMX, and RDX. Some parameters are better. For instance, some parameters of $I\bar{4}m2$ phase of CNO are larger than those of TNT, HMX, and RDX. This compares to values in the range of modern explosives such as TNT, HMX, and RDX, suggesting that these structures have the potential to be high energy density materials.

In summary, we have utilized a combination of the CALYPSO method and first principles calculations to comprehensively investigate the crystal structures of CNO under high pressure. We discovery two novel phases, a $C2/m$ structure and an $I\bar{4}m2$ structure, which are found to be dynamically stable under both high and ambient pressures and exhibit significant potential as HEDMs. Specifically, the $C2/m$ and $I\bar{4}m2$ phase of CNO exhibit energy densities per unit mass of approximately 1.37 kJ/g and 2.70 kJ/g, respectively, which are comparable to those of contemporary explosives, such as TNT, RDX, and HMX. Our findings provide a detailed understanding of the structural evolution and explosive properties of CNO under high pressure, which offer important insights for designs and syntheses of new HEDMs.

Table 3. The explosive properties of ternary $C_xN_yO_z$ compounds and modern explosives, such as TNT, HMX, and RDX.

Compounds	Phase	P_d (kbar)	V_d (km/s)	T(K)	Q (L/kg)	Energy density (kJ/g)	Density (g/cm^3)
CNO	*Pbam*	780	11.4	14700	800	2.2	3.40
	$C2/m$	328	7.9	11355	800	1.4	2.48
	$I\bar{4}m2$	723	11.2	16412	800	2.7	3.11
TNT[5,37–39]	*Pbca*	187	6.9	4095	–	4.2	1.66
TNT	*Pbca*	215	7.1	4172	–	4.2	1.66
HMX[5,37–39]	$P2_1/c$	393	9.1	4867	–	5.7	1.90
HMX	$P2_1/c$	418	9.5	3599	–	5.7	1.90
RDX[37–39]	$Pca2_1$	347	8.8	4909	–	–	1.80
RDX	$Pca2_1$	364	9.1	4902	–	–	1.80
$C_{12}N_8O_{12}$	$Pca2_1$	104	13.0	911	815	3.1	3.62
$C_3N_2O_3$	$Imm2_1$	64	10.6	4756	815	2.1	3.13
$C_4N_2O_4$	$C2/m$	108	13.3	4897	824	3.4	3.59
$C_8N_8O_4$	$Cmc2_1$	75	11.1	1413	640	2.4	3.60

Acknowledgments

This work was supported by the National Natural Science Foundation of China (Grant Nos. 12174352 and 12111530103), the Fundamental Research Funds for the Central Universities, and China University of Geosciences (Wuhan) (Grant No. G1323523065).

References

[1] Raza Z, Pickard C J, Pinilla C and Saitta A M 2013 *Phys. Rev. Lett.* **111** 235501
[2] Goncharov A F, Gregoryanz E, Mao H K, Liu Z X and Hemley R J 2000 *Phys. Rev. Lett.* **85** 1262
[3] Eremets M I, Hemley R J, Mao H K and Gregoryanz E 2001 *Nature* **411** 170
[4] Eremets M I, Gavriliuk A G, Trojan I A, Dzivenko D A and Boehler R 2004 *Nat. Mater.* **3** 558
[5] Hou J, Weng X J, Oganov A R, Shao X, Gao G Y, Dong X, Wang H T, Tian Y J and Zhou X F 2021 *Phys. Rev. B* **103** L060102
[6] Tse J S 2020 *Natl. Sci. Rev.* **7** 149
[7] Gregoryanz E, Goncharov A F, Hemley R J and Mao H K 2001 *Phys. Rev. B* **64** 052103
[8] Huang B W and Frapper G 2018 *Chem. Mater.* **30** 7623
[9] Ding C, Wang J J, Han Y, Yuan J N, Gao H and Sun J 2022 *Chin. Phys. Lett.* **39** 036101
[10] Ding C, Yuan J N, Cogollo-Olivo B H, Wang Y L, Wang X M and Sun J 2023 *Sci. China Phys. Mech.* **66** 228211
[11] Laniel D, Winkler B, Fedotenko T, Pakhomova A, Chariton S, Milman V, Prakapenka V, Dubrovinsky L and Dubrovinskaia N 2020 *Phys. Rev. Lett.* **124** 216001
[12] Miao J Y, Lu Z S, Peng F and Lu C 2021 *Chin. Phys. Lett.* **38** 066201
[13] Hirshberg B, Gerber R B and Krylov A I 2014 *Nat. Chem.* **6** 52
[14] Wang H 2013 *Chin. Phys. B* **22** 086301
[15] Peng F, Yao Y S, Liu H Y and Ma Y M 2015 *J. Phys. Chem. Lett.* **6** 2363
[16] Jiang X X, Chen G Y, Li Y T, Cheng X L and Tang C M 2015 *Chin. Phys. B* **25** 026102
[17] Liu Y, Su H P, Niu C P, Wang X L, Zhang J R, Ge Z X and Li Y C 2020 *Chin. Phys. B* **29** 106201
[18] Yuan J N, Xia K, Ding C, Wang X M, Lu Q and Sun J 2022 *Matter. Radiat. Extrem.* **7** 038402
[19] Zhu C Y, Bi H X, Zhang S T, Wei S B and Li Q 2015 *Rsc. Adv.* **5** 65745
[20] Dai W, He S, Ding K W and Lu C 2022 *Acs. Appl. Mater. Inter.* **14** 49986
[21] Liu L L, Wang D H, Zhang S T and Zhang H J 2021 *J. Mater. Chem. A* **9** 16751
[22] Yoo C S, Kim M, Lim J, Ryu Y J and Batyrev I G 2018 *J. Phys. Chem. C* **122** 13054
[23] Zhu C Y, Li Q, Zhou Y Y, Zhang M, Zhang S T and Li Q 2014 *J. Phys. Chem. C* **118** 27252
[24] Wang Y C, Lv J, Zhu L and Ma Y M 2010 *Phys. Rev. B* **82** 094116
[25] Wang Y C, Lv J, Zhu L and Ma Y M 2012 *Comput. Phys. Commun* **183** 2063
[26] Kresse G and Furthmüller J 1996 *Comp. Mater. Sci.* **6** 15
[27] Duan Q Z, Shen J Y, Zhong X, Lu H Y and Lu C 2022 *Phys. Rev. B* **105** 214503
[28] Sun W G, Chen B L, Li X F, Peng F, Hermann A and Lu C 2023 *Phys. Rev. B* **107** 214511
[29] Tian Y H, Sun W G, Chen B L, Jin Y Y and Lu C 2019 *Chin. Phys. B* **28** 103104
[30] Blöchl P E 1994 *Phys. Rev. B* **50** 17953
[31] Steele B A and Oleynik I I 2017 *Inorg. Chem.* **56** 13321
[32] Mouhat F and Coudert F X 2014 *Phys. Rev. B* **90** 224104
[33] Tang W, Sanville E and Henkelman G 2009 *J. Phys.: Condens. Matter* **21** 084204
[34] Dronskowski R and Blöchl P E 1993 *J. Phys. Chem.* **97** 8617
[35] Steinberg S and Dronskowski R 2018 *Crystals* **8** 225
[36] Fan C Z, Li J and Wang L M 2014 *Sci. Rep.* **4** 1
[37] Yang M, Ma H H and Shen Z W 2019 *J. Energy Mater.* **37** 459
[38] Korkin A A and Bartlett R J 1996 *J. Am. Chem. Soc.* **118** 12244
[39] Kamlet M J and Dickinson C 1968 *J. Chem. Phys.* **48** 43